CONEM 2016
CONGRESSO NACIONAL DE ENGENHARIA MECÂNICA
21 - 25 AGOSTO DE 2016
FORTALEZA - CEARÁ

EVOLUTIONARY TOPOLOGY OPTIMIZATION FOR COMPLIANT MECHANISM DESIGN

Abstract code: CON-2016-1640

Abstract: *Compliant mechanisms are mechanical devices that achieve motion through elastic deformation. They represent a relatively new variety of lightweight structures and their use has been expanded given their advantages over the traditional rigid-body mechanisms. This paper explores a strategy for compliant mechanisms design using the bi-directional evolutionary topology optimization (BESO) method. This procedure requires choosing an objective function that handles motion and loading requirements simultaneously for a given set of input force and desired output displacements. The objective function maximizes the desirable displacement and reduces the formation of hinges at the same time. Sensitivity numbers are found by the objective function variation with respect to the design variables, to be later used in the BESO method to add and remove material until an optimal topology is achieved. The implementation is validated by comparing the results with typical topologies found from previous works. Finally, the influence of the workpiece constraint k_{out} over the final topologies is analyzed. The method could be extended to fluid-actuated mechanisms design by considering pressure loads instead of point loads. This approach will require the implementation of design dependent loads to formulate the optimization problem, an interesting subject to address for further investigations.*
Keywords: *Topology Optimization, BESO, Compliant mechanisms, Multi-criteria Optimization.*

1. INTRODUCTION

A mechanism is defined as a mechanical device used to transmit motion, force or energy and can be classified into two main groups: rigid-body and compliant mechanisms. The compliant or flexible mechanisms gain their mobility by transforming an input form of energy either be mechanical, electric, thermal or magnetic, into output motion (Lobontiu, 2003). The advantages of compliant mechanisms include the possibility to be fabricated from a single layer with no assembly required; they are also compact, do not need lubrication and can be used for applications where high precision and reliability are needed (Howell, 2013).

While the advantages of compliant mechanisms are outstanding, they also have some challenges that have to be carefully considered in their design. For example, integration of different functions into fewer parts offers advantages, but it also requires the simultaneous design for motion and force behavior. This difficulty is increased further by the fact that the deflections are often well into the nonlinear range making her design very difficult to addressed. The complexity of compliant mechanisms elastic behavior has made its design been typically accomplished by trial and error methods (Sigmund, 1997). However, over the past few decades the scientific community has advanced on this matter: New materials, high computational capabilities and new approaches for a more systematic design.

Several systematic methods have been developed to synthesize and design compliant mechanisms. Ananthasuresh and Kota (1995) originally developed a continuum-based approach which uses the techniques of structural optimization and the homogenization method. Sigmund (1997) developed the density method based on the continuum-type topology optimization technique for the optimal design of compliant mechanisms. Nishiwaki *et al.* (1998) adopted the homogenization method for solving optimization problems of compliant mechanisms by introducing a mutual energy concept. Saxena and Ananthasuresh (2001) generalized multi-criteria formulations in terms of monotonically increasing functions of the output deformation and the strain energy. Topology optimization is one of those methods, with the advantage that very little prior knowledge about the resulting compliant mechanism is needed and any biases of the designer are eliminated. Topology optimization is often integrated with finite element methods to consider many possible ways of distributing material with the design domain (Howell, 2013). Some interesting works have been developed using topology optimization such as Cardoso and Fonseca (2006) who designed a strategy to optimize piezoelectric actuators considering geometric nonlinearities using the generalized method of moving asymptotes (GMMA) or Lopes and Novotny (2015) who used the topological derivative to synthesize compliant mechanisms with stress restrictions.

The Evolutionary topology optimization or ESO method is based on a simple concept that inefficient material is gradually removed from the design domain so that the resulting topology evolves towards an optimum. The later version of the BESO method, namely the bi-directional evolutionary topology optimization (BESO), allows not only to remove material from the least efficient regions but also to add material near the most efficient regions simultaneously (Li *et al.*, 2013). The BESO method could be used in several applications, such as problems with fluid structure interaction (Vicente *et al.*, 2015), design dependent loads (Picelli *et al.*, 2014) or porous-acoustic absorbing systems (Silva and Pavanello, 2010). The traditional BESO method is used in this work for the compliant mechanism design using a multi-criteria objective function. For this purpose, the structure strain energy is introduced into the optimization problem formulation as was already made by Li *et al.* (2013). His work is one of the few investigations that used the BESO method for compliant mechanism design and was a very important reference for the development of this investigation. After the BESO method is implemented and the results validated with previous topologies found in the literature, the workpiece constraint (k_{out}) influence is studied and its importance into the problem formulation.

2. OPTIMIZATION FORMULATION

Because required flexibility and stiffness are conflicting design objectives, incorporating both into a single design problem requires two different loading conditions and a multi-criteria optimization strategy (Frecker *et al.*, 1997). The first condition is called "mechanism design" where maximum flexibility is needed. The objective function to accomplish maximum flexibility can be posed as a deflection maximization, or even better, by maximizing a displacement ratio between input and output ports, which is called geometric advantage $GA = u_{out}/u_{in}$. The mechanism design domain can be seen in Fig. 1a, where a general design domain Ω under given loading and boundary conditions is established. The applied force at the input port i is F_{in} and the reaction force at the output j is F_{out} representing the workpiece resistance. F_{out} is modeled by adding a spring with constant stiffness k_{out} at the output port.

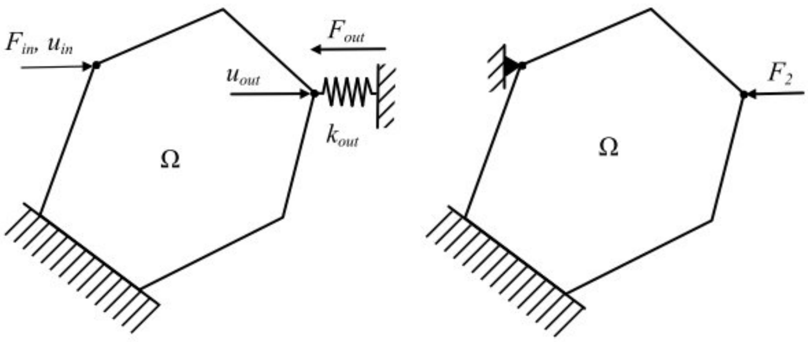

(a) (b)

Figure 1: Generaldesign model for hinge-free compliant mechanism (a) Mechanism design; (b) Structure design;

To formulate the objective function correctly the second loading condition needs to be considered. This new design domain is called "structure design" and is where the structural requirements are met by maximizing the stiffness (Frecker *et al.*, 1997). The compliant mechanism becomes a structure as shown in Fig. 1b when the input port is fixed and a "dummy load" F_2 is applied at the output port, accounting for the workpiece resistance. The boundary conditions stay invariable and the dummy load has the opposite direction to the desired displacement u_{out}. Maximizing the stiffness is equivalent to minimizing the structure compliance, so the second objective function will be $SE = \frac{1}{2}\mathbf{u}^T\mathbf{K}\mathbf{u}$ where $\mathbf{u}$ is the displacement vector for the second loading condition. Maximizing the structural stiffness or minimizing the total strain energy has the advantage that can also preclude the formation of hinges in the compliant mechanism design (Rahmatalla and Swan, 2004).

Now that the two loading conditions and the two objective functions GA and SE are modeled, they need to be combined somehow. The usual multi-criteria approach uses a weighted linear combination, but it's not practical for this particular case: values for both objectives often differ by several orders of magnitude depending on the problem specifications and when this happens, the larger one will dominate (Frecker *et al.*, 1997). An easy way to avoid this problem is the use of a ratio. Since the mutual energy needs to be maximized and the strain energy minimized, the objective function can be formulated as in Eq. (1):

$$\begin{aligned} &\text{Maximize:} && h(x_e) = GA/SE \\ &\text{subject to:} && V^* - \textstyle\sum_{e=1}^{N} V_e x_e = 0 \\ & && x_e = x_{min} \text{ or } 1 \end{aligned} \tag{1}$$

Where $h(x_e)$ denotes the optimization objective function, V_e is the volume of one finite element and V^* represents the structure final volume constraint. The design variable x_e declares the presence of soft elements ($x_e = x_{min}$) or solid ones ($x_e = 1$), according to the soft-killed BESO method used in this work (Huang and Xie, 2010).

To obtain the input and output displacements in order to find GA, the classical approach uses a mechanical analysis where this values can be found by solving equations for two load cases that are later added by the superposition principle (Sigmund, 1997), approach already used by Li (2014). This work proposes a little different strategy to simplify the algorithm calculation, especially for the sensitivity numbers. The difference for this approach lies in the calculation of output/input displacements, but first, two loading conditions will be defined for the finite element analysis and refer to the two structures shown in Fig. 1.

The first case is related to the first loading condition or "mechanism design" illustrated in Fig. 1a. In this case, the superposition principle is not used for the output and input displacement calculation as was made in Li (2014) work. Instead, a spring constant stiffness k_{out} is added to the global stiffness matrix $\mathbf{K}$ at the degree of freedom i_{out} corresponding to the output displacement, as shown in Eq. (2).

$$\mathbf{K}_s(i_{out}, i_{out}) = \mathbf{K}(i_{out}, i_{out}) + k_{out} \tag{2}$$

Where $\mathbf{K}_s$ is the new global stiffness matrix that includes the workpiece constraint influence. The next step is to solve the equilibrium problem $\mathbf{K}_s\mathbf{U}_1 = \mathbf{F}$ to find the displacement vector $\mathbf{U}_1$, with $\mathbf{F}$ being the load vector containing the input force F_{in}. A usual approach to dealing with individual displacements using a virtual load vector is considered to calculate the displacements u_{in} and u_{out}. This load vector has all its components being equal to zero except the one corresponding to the constrained displacement component. The non-zero component is given a unit value at the same direction as the displacement constraint (Xiaoying Yang, 1999). To facilitate the numerical implementation, two virtual load vectors $\mathbf{L}_{in}$ and $\mathbf{L}_{out}$ are created and the individual displacements can be calculated as:

$$\begin{aligned} u_{in} &= \mathbf{L}_{in}\mathbf{U}_1 \\ u_{out} &= \mathbf{L}_{out}\mathbf{U}_1 \end{aligned} \tag{3}$$

The second case or second loading condition is calculated by simply solving the equilibrium equation $\mathbf{K}\mathbf{U}_2 = \mathbf{F}_2$ for the structure in Fig. 1b, with $\mathbf{U}_2$ being the displacement vector for the stiff structure and $\mathbf{F}_2$ the force vector with the dummy load $F_2 = 1$ as the only non-zero component. The displacement vector U_2 found after the finite element analysis is used to calculate the compliance SE for the second loading condition by the expression $SE = \frac{1}{2}\mathbf{U}_2^T\mathbf{K}\mathbf{U}_2$.

Once both loading conditions are solved, the output and input displacements found by Eq. (3) are used to calculate the geometric advantage defined as $GA = u_{out}/u_{in}$. With values for GA and SE, and the help of Eq. (1), the objective function now can be estimated. It is important to observe that this way, only two equilibrium equations need to be solved to find the objective function and the sensitivity numbers.

3. SENSITIVITY ANALYSIS

To find the elemental sensitivity number, the objective function variation with respect to the design variable is needed and can be calculated by deriving Eq. (1).

$$\alpha_e = \left(SE \times \frac{\partial GA}{\partial x_e} - GA \times \frac{\partial SE}{\partial x_e} \right) / SE^2 \tag{4}$$

The sensitivity numbers for the geometric advantage $\partial GA/\partial x_e$ and the compliance $\partial SE/\partial x_e$ are calculated separately to be later included in Eq. (4). We start calculating $\partial GA/\partial x_e$ by deriving equation $GA = u_{out}/u_{in}$

$$\frac{\partial GA}{\partial x_e} = \left(\frac{\partial u_{out}}{\partial x_e} u_{in} - \frac{\partial u_{in}}{\partial x_e} u_{out} \right) / u_{in}^2 \tag{5}$$

The next step in order to find an expression for the geometric advantage sensibility $\partial GA/\partial x_e$ is to find the output and input sensibilities with help from Eq. (3).

$$\begin{aligned} \frac{\partial u_{out}}{\partial x_e} &= \frac{\partial (\mathbf{L}_{out}\mathbf{U}_1)}{\partial x_e} = \mathbf{L}_{out}\frac{\partial \mathbf{U}_1}{\partial x_e} \\ \frac{\partial u_{in}}{\partial x_e} &= \frac{\partial (\mathbf{L}_{in}\mathbf{U}_1)}{\partial x_e} = \mathbf{L}_{in}\frac{\partial \mathbf{U}_1}{\partial x_e} \end{aligned} \tag{6}$$

Deriving the equilibrium equation $\mathbf{K}_s\mathbf{U}_1 = \mathbf{F}$ and reorganizing the terms, the displacement sensitivity $\partial \mathbf{U}_1/\partial x_e$ can be found as shown in Eq. (7).

$$
\begin{aligned}
&\mathbf{K}_s\mathbf{U}_1 = \mathbf{F} \\
&\frac{\partial(\mathbf{K}_s\mathbf{U}_1)}{\partial x_e} = \frac{\partial \mathbf{F}}{\partial x_e} \\
&\frac{\partial \mathbf{K}_s}{\partial x_e}\mathbf{U}_1 + \mathbf{K}_s\frac{\partial \mathbf{U}_1}{\partial x_e} = \frac{\partial \mathbf{F}}{\partial x_e}
\end{aligned} \tag{7}
$$

Considering that the vector $\mathbf{F}$ only contains the load conditions related to the problem design and that those loads do not change with x_e variations, $\partial\mathbf{F}/\partial x_e$ is equal to zero and the expression for $\partial\mathbf{U}_1/\partial x_e$ becomes:

$$
\frac{\partial \mathbf{U}_1}{\partial x_e} = -\mathbf{K}_s^{-1}\frac{\partial \mathbf{K}_s}{\partial x_e}\mathbf{U}_1 \tag{8}
$$

With the expression found in Eq. (8) for $\partial\mathbf{U}_1/\partial x_e$ we can rewrite the expressions for $\partial u_{out}/\partial x_e$ and $\partial u_{in}/\partial x_e$ using Eq.(6).

$$
\begin{aligned}
&\frac{\partial u_{in}}{\partial x_e} = -\mathbf{L}_{in}\mathbf{K}_s^{-1}\frac{\partial \mathbf{K}_s}{\partial x_e}\mathbf{U}_1 = -\mathbf{\Lambda}_{in}\frac{\partial \mathbf{K}_s}{\partial x_e}\mathbf{U}_1 \\
&\frac{\partial u_{out}}{\partial x_e} = -\mathbf{L}_{out}\mathbf{K}_s^{-1}\frac{\partial \mathbf{K}_s}{\partial x_e}\mathbf{U}_1 = -\mathbf{\Lambda}_{out}\frac{\partial \mathbf{K}_s}{\partial x_e}\mathbf{U}_1
\end{aligned} \tag{9}
$$

Where the vectors $\mathbf{\Lambda}_{out}$ and $\mathbf{\Lambda}_{in}$ represent the displacement response to the virtual load vectors $\mathbf{L}_{out}$ and $\mathbf{L}_{in}$. A material interpolation scheme with penalization is used in this work to achieve a nearly solid-void design for the BESO method, a strategy that has been widely used for the SIMP method (Bendsoe, 1989; Bendsoe and Sigmund, 2003; Rubio *et al.*, 2010). The scheme interpolates the Young modulus of the intermediate material as a function of the element density x_e by the expression $E(x_e) = E^0 x_e^p$, with E^0 as the material Young's modulus and p being the penalty exponent. Under this considerations the global stiffness matrix $\mathbf{K}$ can be expressed by the elemental stiffness matrix and design variable x_e as:

$$
\mathbf{K} = \sum_e x_e^p \mathbf{K}_e^0 \tag{10}
$$

Where $\mathbf{K}_e^0$ denotes the elemental stiffness matrix for solid elements. Finally, using equation 10 to derive the global stiffness matrix $\partial\mathbf{K}_s/\partial x_e$ at the elemental level, we obtained all the values needed to calculate the first objective function derivative $\partial GA/\partial x_e$.

$$
\begin{aligned}
&\frac{\partial u_{in}}{\partial x_e} = -p x_e^{(p-1)}\mathbf{\Lambda}_{in,e}\mathbf{K}_e^0\mathbf{U}_{1,e} \\
&\frac{\partial u_{out}}{\partial x_e} = -p x_e^{(p-1)}\mathbf{\Lambda}_{out,e}\mathbf{K}_e^0\mathbf{U}_{1,e}
\end{aligned} \tag{11}
$$

The terms $\mathbf{\Lambda}_{in,e}$ and $\mathbf{\Lambda}_{out,e}$ are the elemental components of the global adjoint vectors $\mathbf{\Lambda}_{out}$ and $\mathbf{\Lambda}_{in}$, in other words, represent the displacement response to the virtual loads for each eth element separately. The output and input displacements sensitivities $\partial u_{out}/\partial x_e$ and $\partial u_{in}/\partial x_e$ can be expressed at elemental levels for solid and soft elements, as two discrete design variables $x_e = 1$ and $x_e = x_{min}$ according to the soft kill BESO method (Huang and Xie, 2010).

$$
\frac{\partial u_{in}}{\partial x_e} = \begin{cases} -p\mathbf{\Lambda}_{in,e}\mathbf{K}_e^0\mathbf{U}_e & \text{when:} \quad x_e = 1 \\ -p x_{min}^{(p-1)}\mathbf{\Lambda}_{in,e}\mathbf{K}_e^0\mathbf{U}_e & \text{when:} \quad x_e = x_{min} \end{cases} \tag{12}
$$

$$
\frac{\partial u_{out}}{\partial x_e} = \begin{cases} -p\mathbf{\Lambda}_{out,e}\mathbf{K}_e^0\mathbf{U}_e & \text{when:} \quad x_e = 1 \\ -p x_{min}^{(p-1)}\mathbf{\Lambda}_{out,e}\mathbf{K}_e^0\mathbf{U}_e & \text{when:} \quad x_e = x_{min} \end{cases} \tag{13}
$$

Replacing this new expressions for $\partial u_{in}/\partial x_e$ and $\partial u_{out}/\partial x_e$ into Eq. (5), the sensitivity number for GA at the elemental level is determined. There is only one step left to find the overall sensitivity number and is to obtained the compliance sensitivity number $\partial SE/\partial x_e$, from the second load case in the structure showed in Fig. 1b. For this propose, the expression $SE = \frac{1}{2}\mathbf{U}_2^T\mathbf{K}\mathbf{U}_2$ is derived as follows:

$$
\frac{\partial SE}{\partial x_e} = -\frac{1}{2}\mathbf{U}_2^T\frac{\partial \mathbf{K}}{\partial x_e}\mathbf{U}_2 = -\frac{1}{2}p x_e^{(p-1)}\mathbf{U}_{2,e}^T\mathbf{K}_e^0\mathbf{U}_{2,e} \tag{14}
$$

Where $\mathbf{U}_{2,e}$ represents the elemental components of the displacement vector U_2 for each eth element. The total strain sensitivity can also be expressed for solid and void elements for the BESO Method accordingly with the material interpolation scheme (Huang and Xie, 2010). With this considerations Eq. (14) stays:

$$\frac{\partial SE}{\partial x_e} = \begin{cases} -\frac{1}{2}p\mathbf{U}_{2,e}^T\mathbf{K}_e^0\mathbf{U}_{2,e} & \text{when:} \quad x_e = 1 \\ -\frac{1}{2}px_{min}^{(p-1)}\mathbf{U}_{2,e}^T\mathbf{K}_e^0\mathbf{U}_{2,e} & \text{when:} \quad x_e = x_{min} \end{cases} \tag{15}$$

4. NUMERICAL IMPLEMENTATION

The traditional BESO method is now implemented for compliant mechanisms design and the whole iteration procedure is outlined as follows:

1. The procedure starts by discretizing the whole design domain using a finite element mesh with given boundary and loading conditions.
2. Define parameters relative to the BESO method such as elemental densities x_e, penalty exponent p and filter radius r_{min}.
3. Perform finite element analysis to find the nodal displacements for the two different load conditions established to satisfy the kinematic and structural requirements. Calculate the sensitivity numbers separately for both objective functions $\partial GA/\partial x_e$ and $\partial SE/\partial x_e$ to obtained the overall sensitivity numbers using equation 4.
4. Update the sensitivity numbers using a filter scheme to prevent unstable phenomena such as checkerboard and mesh-dependency problems.
5. Average the sensitivity number with its historical information to stabilize the evolution process and save it for the next iteration.
6. Determine the target volume for the next iteration according to the evolutionary volume ratio ER. This target volume V_{i+1} can be calculated by $V_{i+1} = V_i(1-ER)$ if the current volume V_i is larger than the objective volume V^*. Otherwise, the target volume for the next design V_{i+1} is set to be $V*$.
7. Rank all elements sensitivity numbers and set the threshold of the sensitivity number,a_{th} so that the total volume of elements with a_{th} so that the total volume of elements with $a_e > a_{th}$ equals to the target volume of the next iteration, V_{i+1}. Then, update the design variables, that is, the elemental density for solid elements is switched from 1 to x_{min} if $a_e \leq a_{th}$ and the elemental density for void elements is switched from x_{min} to 1 if $a_e > a_{th}$.
8. Repeat steps 3-7 until the constraint volume (V^*) is achieved and the objective function is convergent.

5. RESULTS AND DISCUSSION

The BESO algorithm for compliant mechanism design was implemented using MATLAB and validated by comparing the results with topologies found from previous works. For this verification stage, the results from Li (2014) and Li *et al.* (2013) research are used as a reference, given that, as was already mentioned this was one of the few works to apply the BESO method for compliant mechanisms design.

The proposed BESO method is used for an inverter mechanism design shown in Fig. 2a, which outputs the displacement in an opposite direction of the input force. The design domain is 200 mm×200 mm and is discretized with a 100×100 four-node quadrilateral element mesh.

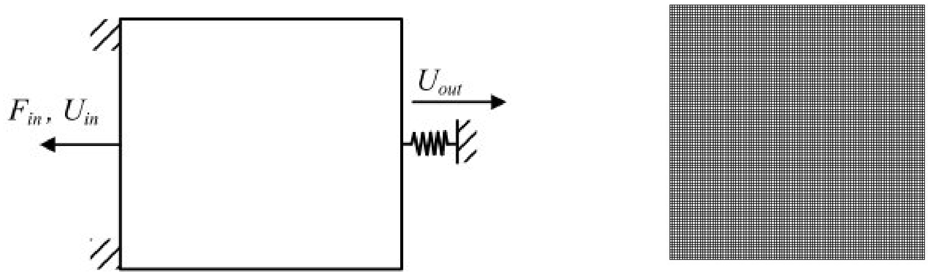

(a) (b)

Figure 2: Design domain and boundary conditions for the Inverter case: (a) Inverter design domain; (b) Finite element mesh for the initial design domain.

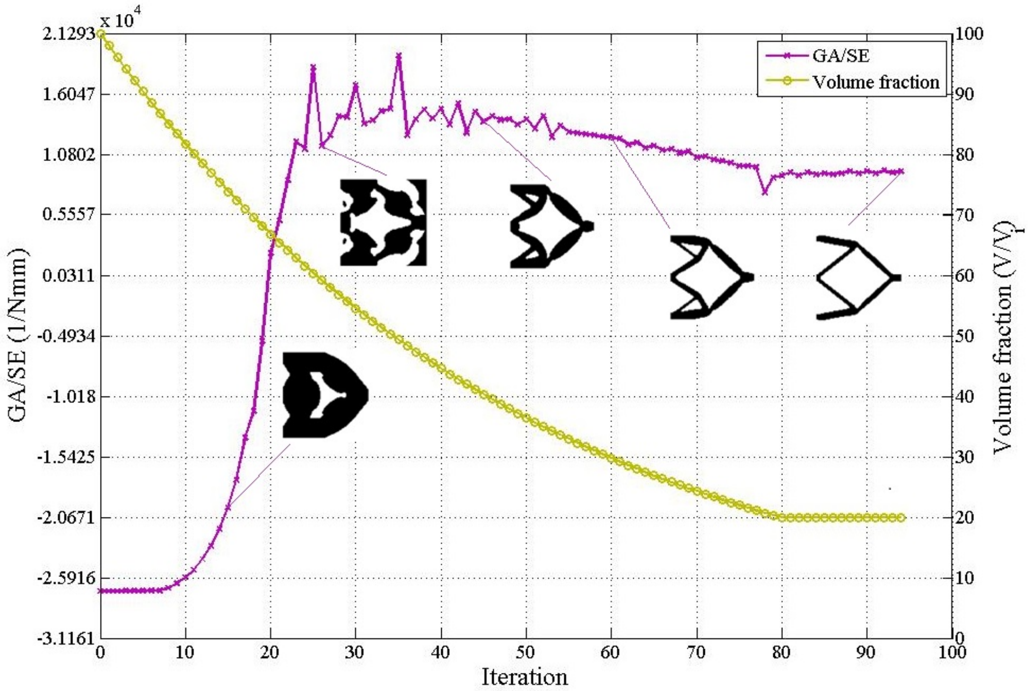

Figure 3: Evolution of the volume fraction and objective function for the inverter mechanism.

The structure is supported at the top and bottom corners of the left edge and an input force $F_{in} = 1N$ is applied at the input port in the horizontal direction. The output port is located at the center of the right edge and is expected to produce a horizontal displacement u_{out} to the right. The material properties are Young's modulus $E = 200GPa$ and Poisson's ratio $\nu = 0.3$. The BESO parameters for this simulation are evolutionary volume ratio $ER = 2\%$, filter radius $r_{min} = 6mm$, penalty exponent $p = 3$, final volume fraction $V_f = 20\%$, convergence tolerance $\tau = 0,1\%$ and $x_{min} = 0.001$.

The evolution of the objective function and the volume fraction can be seen in Fig. 3. The BESO algorithm starts with a full design domain and gradually decreases the volume fraction until it satisfies the $V_f = 20\%$ constraint value at the 80 th iteration. It can also be seen the way the topology evolves during the optimization, with significant changes until the volume constraint is achieved. Beyond this point, the topology remains almost invariable, only reorganizing the elements to fulfill the convergence criteria.

From Fig. 3 we also observed some jumps in the objective function between iterations 20 and 30. Within this range, the topology suffers drastic changes, as can be appreciated for the 25 th iteration. The jumps in the convergence function are related to this dramatic changes, and those variations can be associated to GA and SE individual evolution. Both functions were analyzed separately and was observed that the topology erratic behavior during the optimization process matches the sections where the Compliance SE also fluctuates, showing a strong influence of this variable on the overall objective function.

Besides the common BESO parameters involved in the evolutionary topology optimization such as ER, AR_{max} or r_{min}, there is a new parameter included in the formulation problem for compliant mechanism design: the workpiece constraint k_{out}. This parameter allows to incorporate a restriction at the output port to simulate the workpiece resistance and its estimation depends on the particular application. Its influence on the overall result will be also analyzed.

The analysis was made for the inverter case and the algorithm was tested by varying k_{out} from 0 to the maximum possible value. This upper limit was reached at $k_{out} = 4.9 \times 10^5 N/mm$, beyond this point the structure no longer supports the loading conditions and delivers a disconnected topology. Figure 4 gather the topologies for k_{out} values that had important variations between k_{out} extreme values.

From the different topologies found in 4, there are some important remarks related to the k_{out} variation. First, small alterations in the topology are only perceived after $k_{out} = 20N/mm$, which can be appreciated by comparing figure 4a and 4b, showing that the topology for $k_{out} = 20N/mm$ is almost identical to the topology without any workpiece constraint. Also, the variations occur for high values of k_{out}. Figures 4d and 4e are also almost identical, which implies that after $k_{out} = 2 \times 10^3$ the topology stays invariable until its maximum value.

After examining the different topologies in Fig.4, it could be concluded that for this particular case, the workpiece constant stiffness k_{out} does not radically affect the final topology and the variations are observed only for large increases in k_{out}. This could be explained by the objective function formulation: when the compliance SE was included in the optimization problem, every possible structure will fulfill the stiffness requirement, making the structure strong enough to support any external load. This way k_{out} is not the only parameter that considers the workpiece resistance, preventing its direct influence over the final topology. Without the SE condition, the variable k_{out} will be necessarily different from zero to account for the workpiece resistance and to ensure a well-conditioned problem.

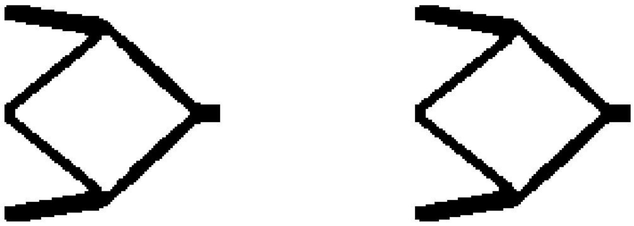

(a) (b)

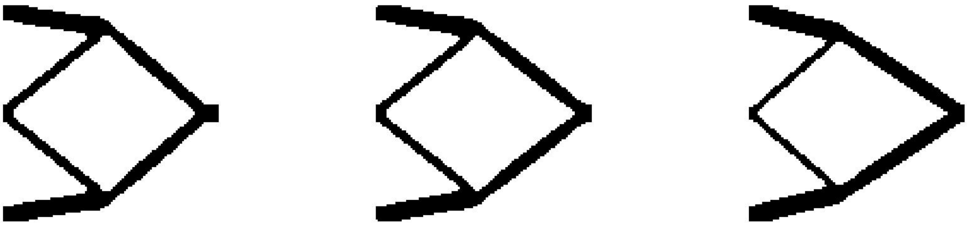

(c) (d) (e)

Figure 4: Optimal topologies for the inverter case with different constant stiffness (a) $k_{out} = 0$. (b) $k_{out} = 200$. (c) $k_{out} = 2 \times 10^3$.(d) $k_{out} = 2 \times 10^4$. (e) $k_{out} = 4.9 \times 10^5$

6. CONCLUSIONS

This paper uses the bi-directional evolutionary topology optimization method (BESO) to the compliant mechanisms design, using a multicriteria strategy to formulate the optimization problem. The new objective function incorporates the flexibility condition by maximizing the mechanisms geometric advantage and also fulfills the stiffness requirement by minimizing the structure compliance. The final topology generates a displacement at the output port in the opposite direction of the input force, as was expected, which indicates that the algorithm implemented can be trustfully used in compliant mechanisms design.

The workpiece constraint influence over the inverter final topologies was also studied by increasing the k_{out} value from 0 to the maximum value bearable for the structure. Those k_{out} variations do influence the final topology but only for k_{out} high variations and those changes are not necessarily drastic depending on the particular case. However, by increasing the k_{out} value, the structure also becomes stiffer with every new increase, which is inconvenient considering that the structure also needs to fulfill the flexibility requirement. It is advisable to maintain k_{out} in a low value to avoid an excessive structure stiffness.

7. ACKNOWLEDGMENTS

This work was supported by the National Council for Scientific and Technological Development (CNPq) and Sâo Paulo Research Foundation - FAPESP [grant 2013/08293-7].

8. REFERENCES

Ananthasuresh, G. and Kota, S., 1995. "Designing compliant mechanisms". *Mechanical Engeneering*, Vol. 117, No. 11, pp. 93–96.

Bendsoe, M.P., 1989. "Optimal shape design as a material distribution problem". *Structural Optimization*, Vol. 1, pp. 192–202.

Bendsoe, M.P. and Sigmund, O., 2003. *Topology Optimization - Theory, Methods and Applications*. Springer Verlag, Berlin Heidelberg.

Cardoso, E.L. and Fonseca, J.S.O., 2006. "Topology optimization of piezoelectric actuators considering geometric non-linearities". In *IUTAM Symposium on TOpological Design Optimization of Structures, Machines and Materials*. pp. 391–400.

Frecker, M., Ananthasuresh, G.K., Nishiwaki, S., Kikuchi, N. and Kota, S., 1997. "Topological synthesis of compliant mechanisms using multi-criteria optimization". *Journal of Mechanical Design*, Vol. 119, pp. 238–245.

Howell, L.L., 2013. *2st Century Kinematics*, Springer London, chapter Compliant Mechanism, pp. 189–216.

Huang, X. and Xie, M., 2010. *Evolutionary Topology Optimization of Continuum Structures: Methods and Applications*. Wiley.

Li, Y., Huang, X., Xie, Y. and Zhou, S., 2013. "Evolutionary topology ioptimization of hinge-free compliant mechanisms". *International Journal of Mechanical Sciences*, Vol. 86, pp. 69–75.

Li, Y., 2014. *Topology Optimization of Compliant Mechanics Based on the BESO Method*. Ph.D. thesis, School of Civil - Enviromental and Chemical Engeneering - RMIT University.

Lobontiu, N., 2003. *Compliant Mechanisms - Design of Flexure Hinges*. CRC PRESS.

Lopes, C.G. and Novotny, A.A., 2015. "Síntese de mecanismos flexíveis com restrição em tensão utilizando o conceito de derivada topologica." In *XXXI Ibero-Latin American Congress on Computational Methods in Engeneering - CILAMCE*.

Nishiwaki, S., Frecker, M.I., Min, S. and Kikuchi, N., 1998. "Topology optimization of compliant mechanisms using the homogenization method". *International Journal for Numerical merhods in engeneering*, Vol. 42, pp. 535–559.

Picelli, R., Vicente, W. and Pavanello, R., 2014. "Bi-directional evolutionary structural optimization for design-dependent fluid pressure loading problems." *Engineering Optimization*, Vol. 47, No. 10, pp. 1324–1342.

Rahmatalla, S. and Swan, C., 2004. "Sparse monolithic compliant mechanisms using structural topology optimization". *International Journal for Numerical Methods in Engineering*, Vol. 62, No. 12, pp. 1579–1605.

Rubio, W.M., Nishiwaki, S. and Silva, E.C.N., 2010. "Design of compliant mechanisms considering thermal effect compensation and topology optimization". *Finite ELements in Analysis and Design*, Vol. 46, No. 12, pp. 1049–1060.

Saxena, A. and Ananthasuresh, K., 2001. "Topology optimization of compliant mechanisms with strength considerations". *Mechanics of Structures and Machines*, Vol. 29, No. 2, pp. 199–221.

Sigmund, O., 1997. "On the design of compliant mechanisms using topology optimization". *Mechanics of Structures and Machines: An International Journal*, , No. 25, pp. 493–524.

Silva, F. and Pavanello, R., 2010. "Synthesis of porous-acustic absorbing systems by an evolutionary optimization method". *Engineering Optimization*, Vol. 42, No. 10, pp. 887–905.

Vicente, W., Picelli, R., Pavanello, R. and Xie, Y., 2015. "Topology optimization of frecuency responses of fluid-structure interaction systems". *Finite Elements in Analysis and Design*, Vol. 98, pp. 1–13.

Xiaoying Yang, B., 1999. *Bi-directional Evolutionary Method for Stiffness and Displacement Optimization*. Master's thesis, School of the Built Enviroment - Victoria University of Technology.

9. AUTHORIAL RESPONSABILITIES

The authors are solely responsible for the content of this work.